Journal of Nuclear Medicine, published on February 26, 2021 as doi:10.2967/jnumed.120.258434

Head to head comparison of ^{68}Ga-NGUL and ^{68}Ga-PSMA-11 in patients with metastatic prostate cancer: a prospective study

Minseok Suh[1,2], Hyung-Jun Im[2,3], Hyun Gee Ryoo[1,2], Keon Wook Kang[1], Jae Min Jeong[1], Sneha Kumar[4], Sanjana Ballal[4], Madhav P Yadav[4], Chandrasekhar Bal[4], Chang Wook Jeong[5], Cheol Kwak[5], Gi Jeong Cheon[1,6,*]

[1]*Department of Nuclear Medicine, Seoul National University College of Medicine, Seoul, Korea*

[2]*Department of Molecular Medicine and Biopharmaceutical Sciences, Graduate school of Convergence Science and Technology, Seoul National University, Seoul, Korea*

[3]*Department of Applied Bioengineering, Graduate School of Convergence Science and Technology, Seoul National University, Seoul, Korea*

[4]*Department of Nuclear Medicine, AIIMS, New Delhi, India*

[5]*Department of Urology, Seoul National University College of Medicine, Seoul, Korea*

[6]*Cancer Research Institute, Seoul National University, Institute on Aging, Seoul National University, Seoul Korea*

[First Authors]

Minseok Suh, MD, PhD
Research Professor

Department of Nuclear Medicine, Seoul National University College of Medicine,
101 Daehak-ro, Jongno-gu, Seoul 03080, Korea

Hyung-Jun Im, MD, PhD
Assistant Professor
Department of Applied Bioengineering

Graduate School of Convergence Science and Technology
Seoul National University
Seoul, Korea

[Corrensponding author]*

Gi Jeong Cheon, MD, PhD
Professor and Chairman
Department of Nuclear Medicine, Seoul National University College of Medicine
101 Daehak-ro, Jongno-gu, Seoul 03080, Korea

Cancer Research Institute, Seoul National University, Institute on Aging, Seoul National University, Seoul, Korea
E-mail: larrycheon@gmail.com, Tel: +822-2072-3386, Fax: +822-745-7690

[Financial Support]

This work was supported by the National Research Foundation of Korea (NRF) grant funded by the Korea government (MSIT) (NRF-2020R1A2C2011428), Korea Health Technology R&D Project through the Korea Health Industry Development Institute (HI18C1916, HI19C0339), and Creative-Pioneering Researchers Program through Seoul National University (SNU).

This work was supported by the Technology Innovation Program (20001235, Development of Novel Radiopharmaceutical for Prostate Cancer Targeted Imaging Diagnosis) funded By the Ministry of Trade, industry & Energy (MI, Korea)

[Word Count] 2602

[Running Title] Comparison of ^{68}Ga-NGUL and ^{68}Ga-PSMA-11

ABSTRACT

Introduction ^{68}Ga-NOTA Glu-Urea-Lys (NGUL) is a novel prostate-specific membrane antigen (PSMA) targeting tracer used for PET/CT imaging. This study aims to compare the performance in the detection of primary and metastatic lesions, and to compare biodistribution between ^{68}Ga-NGUL and ^{68}Ga-PSMA-11 in the same patients with prostate cancer. **Methods** Eleven patients with metastatic prostate cancer were prospectively recruited. The quantitative tracer uptake was obtained in normal organs and, primary and metastatic lesions. **Results** ^{68}Ga-NGUL showed significantly lower normal organ uptake and rapid urinary clearance. The number and sites of detected PSMA positive primary and metastatic lesions were identical and no significant quantitative uptake difference was observed. ^{68}Ga-NGUL showed a relatively lower tumor-to-background ratio than ^{68}Ga-PSMA-11. **Conclusion** In head to head comparison with ^{68}Ga-PSMA-11, ^{68}Ga-NGUL showed lower uptake in normal organs with similar performance to detect PSMA avid primary and metastatic lesions. ^{68}Ga-NGUL could be a valuable option for PSMA imaging.

Keywords: Prostate-specific membrane antigen, ^{68}Ga-NGUL, ^{68}Ga-PSMA-11, biodistribution

INTRODUCTION

Prostate-specific membrane antigen (PSMA), a transmembrane protein overexpressed in prostate cancer, has been one of the most highlighted targets for imaging and therapy of prostate cancer (*1,2*). Among many PSMA PET tracers, ^{68}Ga-PSMA-11, is the most extensively investigated and well-established tracer (*3*). ^{68}Ga-PSMA-11 is superior than conventional imaging modalities in staging and detection of biochemical failure in patients with prostate cancer (*4-7*).

We recently have developed a novel PSMA targeting tracer based on Glu-Urea-Lys (GUL) derivatives, conjugated with NOTA chelator via a thiourea-type short linker, named ^{68}Ga-NOTA-GUL (NGUL) (*8*). In our previous study, ^{68}Ga-NGUL showed a higher tumor to background ratio, and substantially lower kidney uptake than ^{68}Ga-PSMA-11 in PSMA positive tumor xenografted mice (*8*).

To further investigate the clinical feasibility of ^{68}Ga-NGUL, we have conducted a prospective head to head comparison study between ^{68}Ga-NGUL and ^{68}Ga-PSMA-11 PET/CT. The specific aims of this study are to compare the detection efficacy and biodistribution between ^{68}Ga-NGUL and ^{68}Ga-PSMA-11 in the same patients with metastatic prostate cancer.

MATERIALS AND METHODS

Subjects

Patients with metastatic prostate cancer were prospectively recruited in this study. Each patient underwent ^{68}Ga-NGUL and ^{68}Ga-PSMA-11 scans. The quality was assessed before administration, and as a result, ^{68}Ga-NGUL showed high purity and stability (Supplementary Figure 1). This study was approved by the Institutional Review Board. All patients gave written informed consent to have two consecutive PSMA targeted PET/CT scan. All procedures performed in this study were in accordance with the ethical standards of the institutional research committee and with the 1964 Helsinki declaration and its later amendments or comparable ethical standards.

Image acquisition and analysis

The PET/CT scans were performed at 60 minutes after tracer injection. Any focal accumulation of ^{68}Ga-NGUL and ^{68}Ga-PSMA-11 not explained by physiologic uptake were defined as pathologic lesions. Lesion numbers and lesion uptake, as SUV_{max}, were compared (Supplementary Figure 2A). The quantitative tracer uptakes were obtained in normal organs including salivary glands, liver, spleen, and

kidney and blood pool activity was measured in the inferior vena cava (Supplementary Figure 2B). The normal organ distribution of both tracers was quantified as SUV_{mean}. In addition, three patients underwent dynamic PET/CT scanning (60 min) of the pelvic region to evaluate the urinary clearance.

Statistical Analysis

Statistical analyses were performed using PRISM version 5.0 (GraphPad Software, San Diego, CA, USA) and the MedCalc statistical packages version 14.8 (MedCalc Statistical Software, Mariakerke, Belgium). Shapiro-Wilk test was used to evaluate data normality. A comparison between the two tracers was done using Wilcoxon signed-rank test, linear regression, and Bland-Altman analysis.

RESULTS

Eleven patients were prospectively enrolled in the study. The patients' characteristics are summarized in Supplementary Table 1. The time interval between ^{68}Ga-NGUL and ^{68}Ga-PSMA-11 PET/CT scan was 1 to 4 days and no patient received any treatment between both scans. Quantitative data are expressed as the median and interquartile range.

Normal organ distribution

Overall, both scans showed similar distribution patterns with the highest uptake in the kidneys (Fig. 1). An intra-patient comparison using quantitative value revealed significantly different organ uptake in both scans. The SUV_{mean} in the kidneys, salivary glands, spleen, and liver, was significantly lower on ^{68}Ga-NGUL compared with ^{68}Ga-PSMA-11 (Supplementary Table 2, Fig. 1). Linear correlation and agreement between ^{68}Ga-NGUL and ^{68}Ga-PSMA-11 are demonstrated in Supplementary Table 2 and Supplementary Figure 3.

From the dynamic PET imaging, the time-activity curve of the bladder was obtained for both tracers (Fig. 2). Over time, higher bladder retention was observed with ^{68}Ga-NGUL, reflecting more rapid urinary clearance than ^{68}Ga-PSMA-11.

Analysis of primary and metastatic lesions

^{68}Ga-NGUL and ^{68}Ga-PSMA-11 could detect primary lesions in all patients (n =11). There was no

significant difference between the SUVmax of primary tumor (Fig. 3A, Supplementary Table 2).

In a total of 11 patients, 161 nodal and 59 bone PSMA avid metastases were identified. All lesions were detected identically by both tracers and there was no lesion detected only by either ^{68}Ga-NGUL or ^{68}Ga-PSMA-11 (Supplementary Table 3). Quantitative uptake was evaluated in a total of 36 lesions (20 lymph nodes, and 16 bone metastases), which were selected up to a maximum of five lesions (and a maximum of two lesions per organ) in each patient. No significant difference of lymph node and bone metastases uptake were observed between ^{68}Ga-NGUL and ^{68}Ga-PSMA-11 (Fig. 3A, Supplementary Table 2). Linear correlation and agreement between ^{68}Ga-NGUL and ^{68}Ga-PSMA-11 are demonstrated in Supplementary Table 2 and Supplementary Figure 4. The tumor-to-background ratio of ^{68}Ga-NGUL tended to be lower than that of ^{68}Ga-PSMA-11 in primary tumors (37.5 (26.8 – 62.8) vs 58.3 (33.5 – 90.4); p = 0.067) and lymph node metastases (29.7 (18.5 – 55.9) vs 48.1 (12.5 – 99.1); p = 0.114), and the difference was statistically significant in case of bone metastases (48.7 (29.1 – 61.9) vs 81.0 (25.7 – 97.8); p = 0.007) (Fig. 3B).

DISCUSSION

We found that ^{68}Ga-NGUL showed lower uptake in the normal organs including the kidneys, salivary glands, spleen, and liver. ^{68}Ga-NGUL also showed more rapid clearance through the urinary system than ^{68}Ga-PSMA-11. There was no significant difference for absolute lesion uptake, however, ^{68}Ga-NGUL tended to show a lower tumor-to-background ratio compared to ^{68}Ga-PSMA-11. Still, the ability to detect primary and metastatic lesions between ^{68}Ga-NGUL and ^{68}Ga-PSMA-11 was identical.

Several biodistribution studies of ^{68}Ga-PSMA-11 have well demonstrated the cellular expression of PSMA throughout the body, in parts of the lacrimal glands and major salivary glands, liver, spleen, kidneys, and intestines (*9,10*). In this study, ^{68}Ga-NGUL showed a visually similar distribution pattern compared with ^{68}Ga-PSMA-11. However, clearance via the urinary tract was more rapid in ^{68}Ga-NGUL than ^{68}Ga-PSMA-11. Also, normal organ uptake of ^{68}Ga-NGUL in the kidney, liver, salivary glands, and spleen were significantly lower compared to ^{68}Ga-PSMA-11. Several factors, including hydrophilicity, small molecular size, and low protein binding property, could explain the rapid clearance of ^{68}Ga-NGUL (*11,12*). NGUL has a lower molecular weight (769.82 vs. 947 g/mol) and higher hydrophilicity (log P = -3.3 vs. -3.9) than PSMA-11 (Supplementary Figure 5). Indeed, as a diagnostic imaging agent, early clearance of the ^{68}Ga-NGUL through the kidney to the bladder may interfere with the detection of lesions adjacent to the urinary tract. In order to overcome this limitation, proper hydration and post-void delayed scan should be considered in future imaging protocol for ^{68}Ga-NGUL.

Despite the faster clearance of ^{68}Ga-NGUL, there was a trend of a lower tumor-to-background ratio. In our previous study, the binding affinity of ^{68}Ga-NGUL was 18.3nM (*8*), which is relatively lower than that of ^{68}Ga-PSMA-11, reported to be 24.3nM (*13*). Thus, it is speculated that the fraction of the unbound ^{68}Ga-NGUL is relatively higher and ^{68}Ga-NGUL taken up by normal organs or tumor is relatively lower compared to the ^{68}Ga-PSMA-11. As a result, the difference in the tumor-to-background ratio becomes more pronounced.

Some limitations should be noted. Firstly, due to a small number of patients, we cannot allow a generalized conclusion. However, as a head to head comparison study, the difference between the distribution of the two compounds seems to be solid. Nonetheless, further studies with a larger number of patients are needed to validate our findings. Secondly, our cohort does not have whole-body PET data of multiple time points. As a result, we were unable to assess the clinical dose difference between the two agents. However, the effective dose measured from the animal experiments was 0.019 mSv/MBq (Supplementary Table 4), which is similar to the dosimetry data provided by ^{68}Ga PSMA-11 clinical studies. Lastly, the PSA level was not considered comprehensively. As PSMA-avid tumor burden significantly correlates to PSA levels, it is considered to be a good indicator to reflect the tumor status at each scan time points (*4,14*). However, since the term between two scans was short, within 4 days, we speculate that the difference of tumor status in each imaging point is negligible.

CONCLUSION

Head to head comparison of ^{68}Ga-NGUL and ^{68}Ga-PSMA-11 revealed that ^{68}Ga-NGUL showed lower uptake in the normal organs including the kidneys, salivary glands, spleen, and liver, and more rapid clearance through the urinary system. Although, ^{68}Ga-NGUL showed a trend of low tumor-to-background ratio, its ability to detect primary and metastatic lesions was the same as that of ^{68}Ga-PSMA-11. Therefore, ^{68}Ga-NGUL could be a valuable option for PSMA PET/CT imaging.

DISCLOSURE

This work was supported by the National Research Foundation of Korea (NRF) grant funded by the Korea government (MSIT) (NRF-2020R1A2C2011428), Korea Health Technology R&D Project through the Korea Health Industry Development Institute (HI18C1916, HI19C0339), and Creative-Pioneering Researchers Program through Seoul National University (SNU).

This work was supported by the Technology Innovation Program (20001235, Development of Novel Radiopharmaceutical for Prostate Cancer Targeted Imaging Diagnosis) funded By the Ministry of Trade, industry & Energy (MI, Korea)

NGUL kit vial was provided by Cellbion Co., Ltd. (Seoul, Korea).

Hyung-Jun Im MD, PhD is a consultant for Cellbion.

No other potential conflicts of interest relevant to this article exist.

ACKNOWLEDGMENTS

None

KEY POINTS

Questions How does ^{68}Ga-NGUL PET/CT perform in comparison to ^{68}Ga-PSMA-11 in patients with metastatic prostate cancer?

Pertinent Findings We found that the ^{68}Ga-NGUL showed lower uptake in the normal organs and more rapid clearance than ^{68}Ga-PSMA-11. ^{68}Ga-NGUL tended to show lower tumor-to-background ratio compared to ^{68}Ga-PSMA-11. Still the ability to detect primary and metastatic lesions between ^{68}Ga-NGUL and ^{68}Ga-PSMA-11 was identical and no significant difference with respect to lesion uptake was observed.

Implication for patient care ^{68}Ga-NGUL can be a valuable option for metastatic prostate cancer patient imaging and theranostics.

REFERENCES

1. Iravani A, Violet J, Azad A, Hofman MS. Lutetium-177 prostate-specific membrane antigen (PSMA) theranostics: practical nuances and intricacies. *Prostate Cancer Prostatic Dis.* 2020;23:38-52.

2. Siva S, Udovicich C, Tran B, Zargar H, Murphy DG, Hofman MS. Expanding the role of small-molecule PSMA ligands beyond PET staging of prostate cancer. *Nat Rev Urol.* 2020;17:107-118.

3. Eder M, Schafer M, Bauder-Wust U, et al. ^{68}Ga-complex lipophilicity and the targeting property of a urea-based PSMA inhibitor for PET imaging. *Bioconjug Chem.* 2012;23:688-697.

4. Ceci F, Uprimny C, Nilica B, et al. ^{68}Ga-PSMA PET/CT for restaging recurrent prostate cancer: which factors are associated with PET/CT detection rate? *Eur J Nucl Med Mol Imaging.* 2015;42:1284-1294.

5. Fendler WP, Eiber M, Beheshti M, et al. ^{68}Ga-PSMA PET/CT: Joint EANM and SNMMI procedure guideline for prostate cancer imaging: version 1.0. *Eur J Nucl Med Mol Imaging.* 2017;44:1014-1024.

6. Eiber M, Maurer T, Souvatzoglou M, et al. Evaluation of hybrid ^{68}Ga-PSMA ligand PET/CT in 248 patients with biochemical recurrence after radical prostatectomy. *J Nucl Med.* 2015;56:668-674.

7. Hofman MS, Lawrentschuk N, Francis RJ, et al. Prostate-specific membrane antigen PET-CT in patients with high-risk prostate cancer before curative-intent surgery or radiotherapy (proPSMA): a prospective, randomised, multicentre study. *The Lancet.* 2020;395:1208-1216.

8. Moon SH, Hong MK, Kim YJ, et al. Development of a Ga-68 labeled PET tracer with short linker for prostate-specific membrane antigen (PSMA) targeting. *Bioorg Med Chem.* 2018;26:2501-2507.

9. Afshar-Oromieh A, Malcher A, Eder M, et al. PET imaging with a [^{68}Ga]gallium-labelled PSMA ligand for the diagnosis of prostate cancer: biodistribution in humans and first evaluation of tumour lesions. *Eur J Nucl Med Mol Imaging.* 2013;40:486-495.

10. Prasad V, Steffen IG, Diederichs G, Makowski MR, Wust P, Brenner W. Biodistribution of [^{68}Ga]PSMA-HBED-CC in Patients with Prostate Cancer: Characterization of Uptake in Normal Organs and Tumour Lesions. *Mol Imaging Biol.* 2016;18:428-436.

11. Di L. Strategic approaches to optimizing peptide ADME properties. *AAPS J.* 2015;17:134-143.

12. Varma MV, Feng B, Obach RS, et al. Physicochemical determinants of human renal clearance. *J Med Chem.* 2009;52:4844-4852.

13. Kelly J, Amor-Coarasa A, Nikolopoulou A, et al. Synthesis and pre-clinical evaluation of a new class of high-affinity ^{18}F-labeled PSMA ligands for detection of prostate cancer by PET imaging. *Eur J Nucl Med Mol Imaging.* 2017;44:647-661.

14. Schmidkonz C, Cordes M, Schmidt D, et al. ^{68}Ga-PSMA-11 PET/CT-derived metabolic parameters for determination of whole-body tumor burden and treatment response in prostate cancer. *Eur J Nucl Med Mol Imaging.* 2018;45:1862-1872.

Figure legends

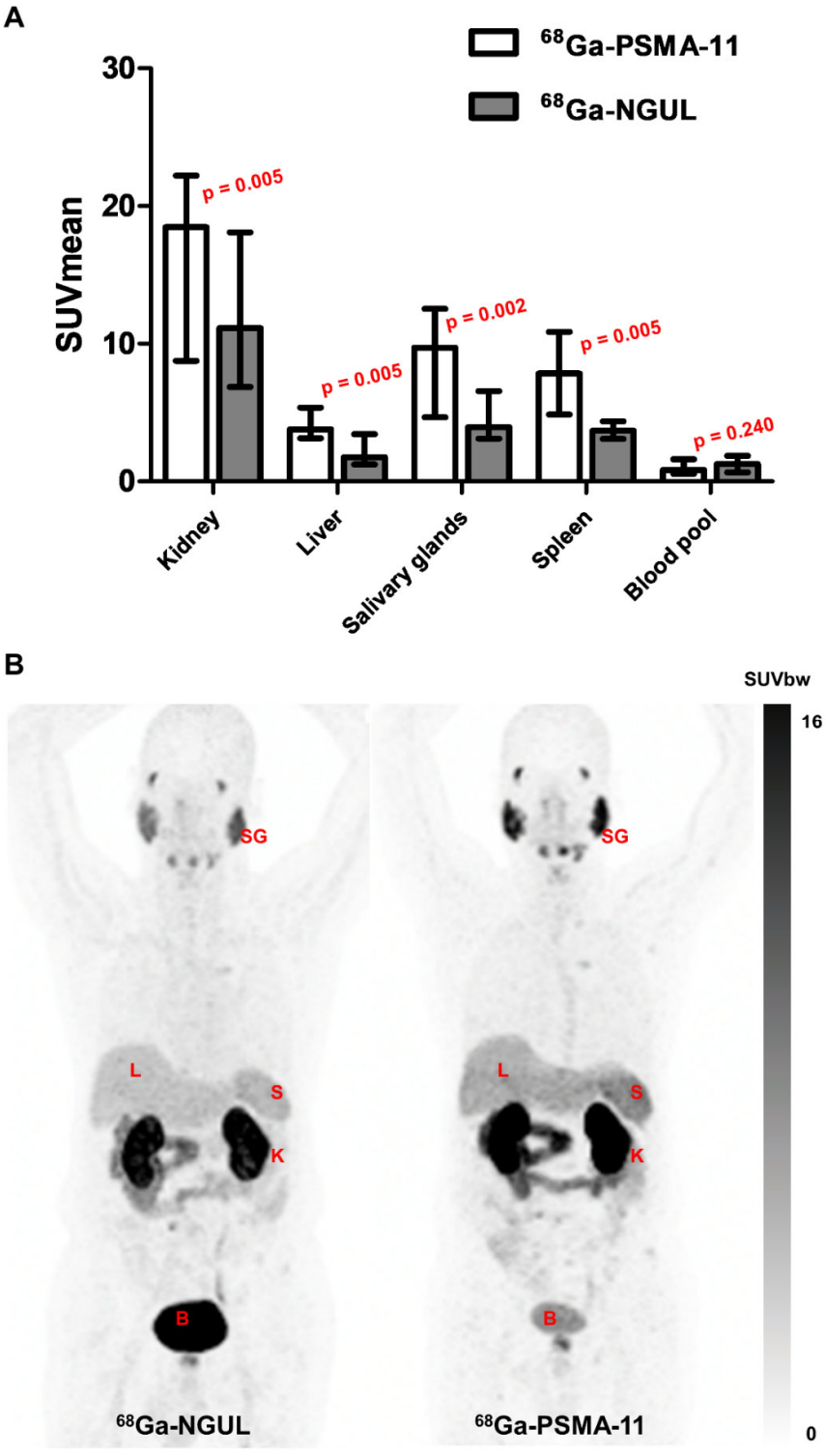

Figure 1

(A) SUV_{mean} value of normal organs for ^{68}Ga-PSMA-11 and ^{68}Ga-NGUL. Median with the interquartile range as an error bar was plotted on the bar chart. Wilcoxon signed-rank test for paired data was used for statistical comparison. (B) Representative image showing normal organ distribution of ^{68}Ga-PSMA-11 and ^{68}Ga-NGUL. (SG, salivary glands; L, liver; S, spleen; K, kidney; B, bladder)

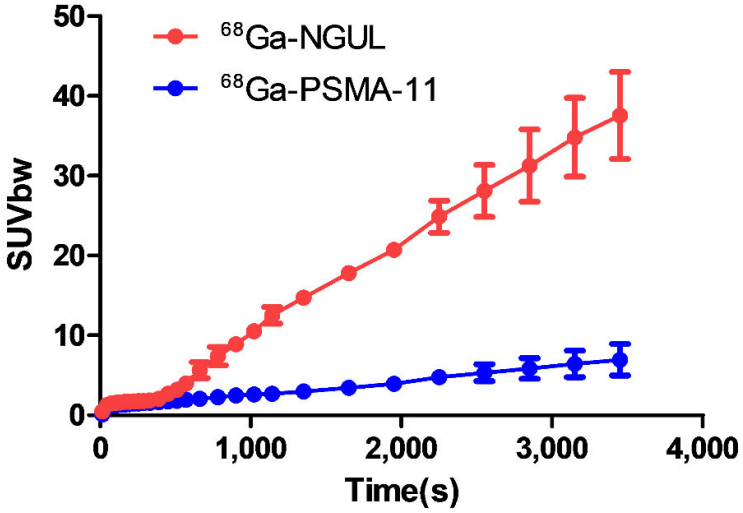

Figure 2

Time-activity curve of both ^{68}Ga-PSMA-11 and ^{68}Ga-NGUL derived from bladder region of interest.

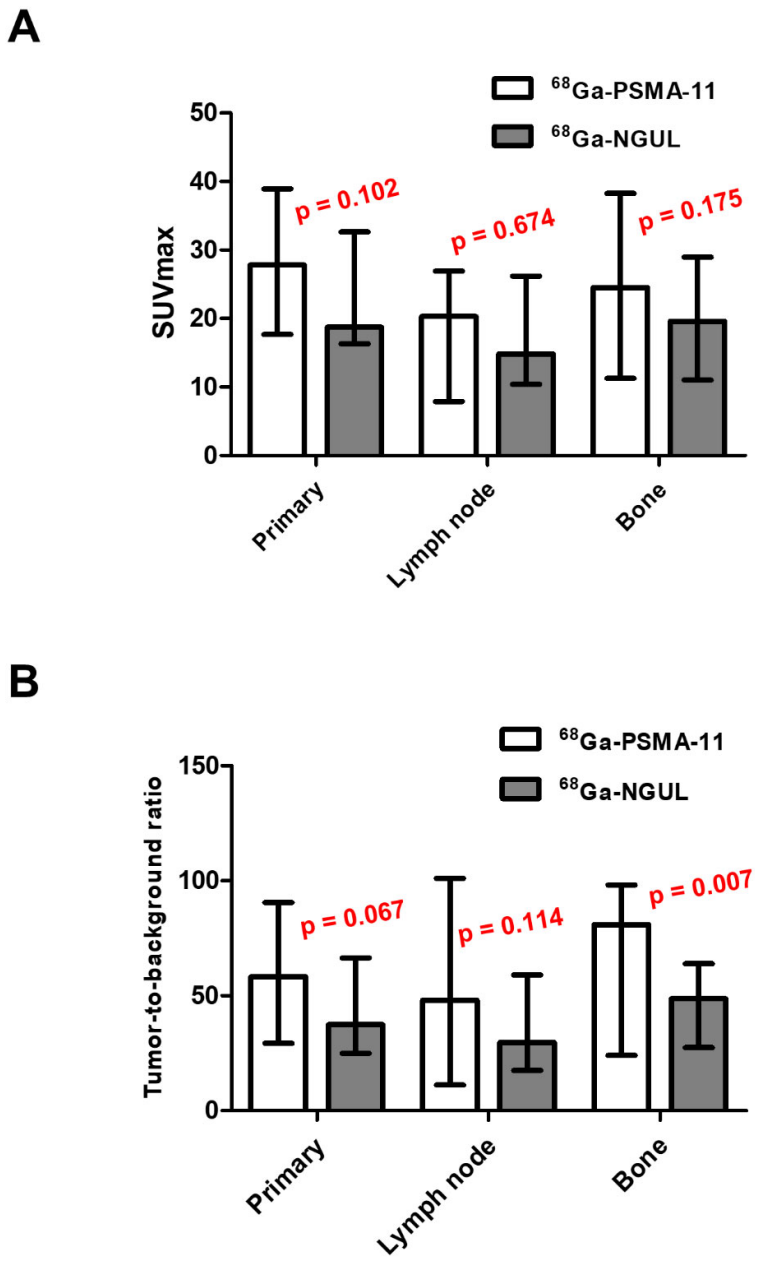

Figure 3

(A) SUV_{max} value of primary tumor, lymph node, and bone metastases for ^{68}Ga-PSMA-11 and ^{68}Ga-NGUL. (B) Tumor-to-background ratio of the primary tumor, lymph node, and bone metastases for ^{68}Ga-PSMA-11 and ^{68}Ga-NGUL. Median with the interquartile range as an error bar was plotted on the bar chart. Wilcoxon signed-rank test for paired data was used for statistical comparison.

Graphical abstracts

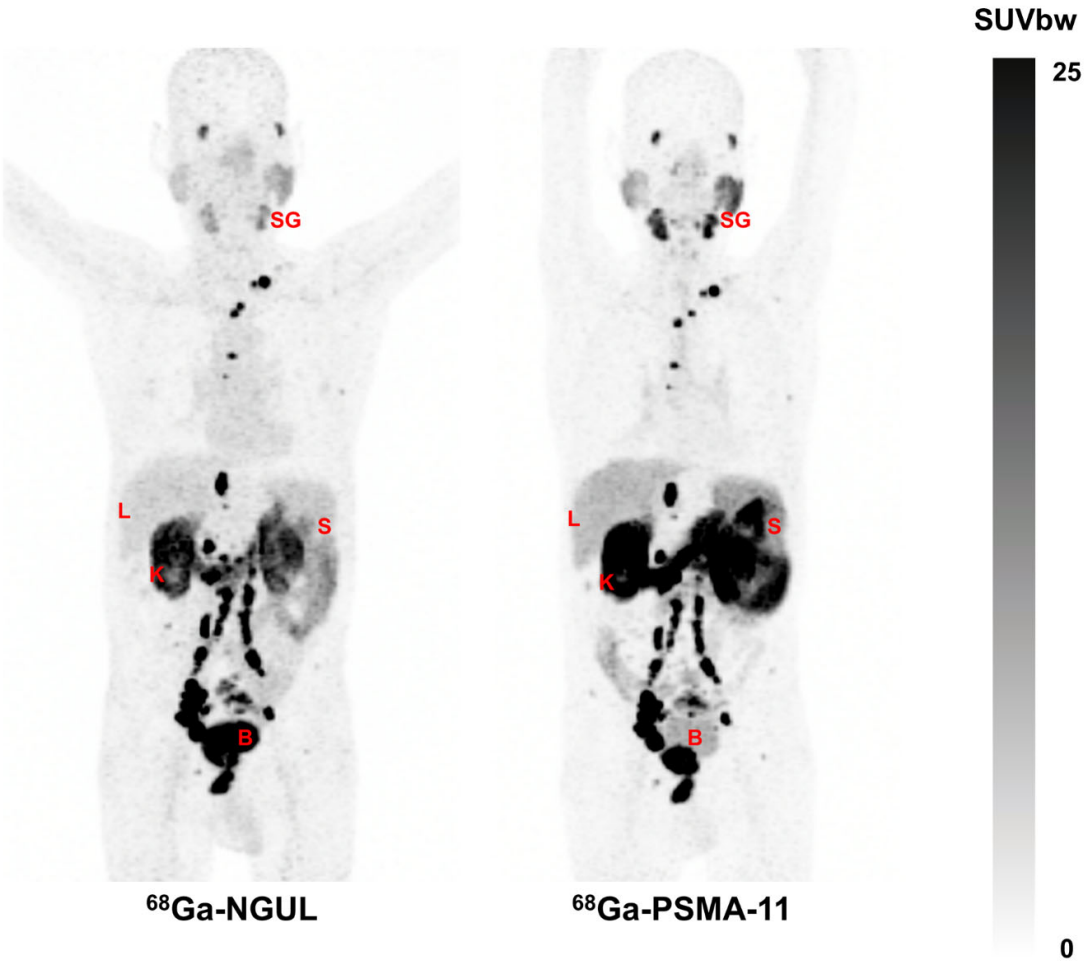

Supplementary Data

Head to head comparison of ^{68}Ga-NGUL and ^{68}Ga-PSMA-11 in patients with metastatic prostate cancer: a prospective study

SUPPLEMENTARY FIGURES

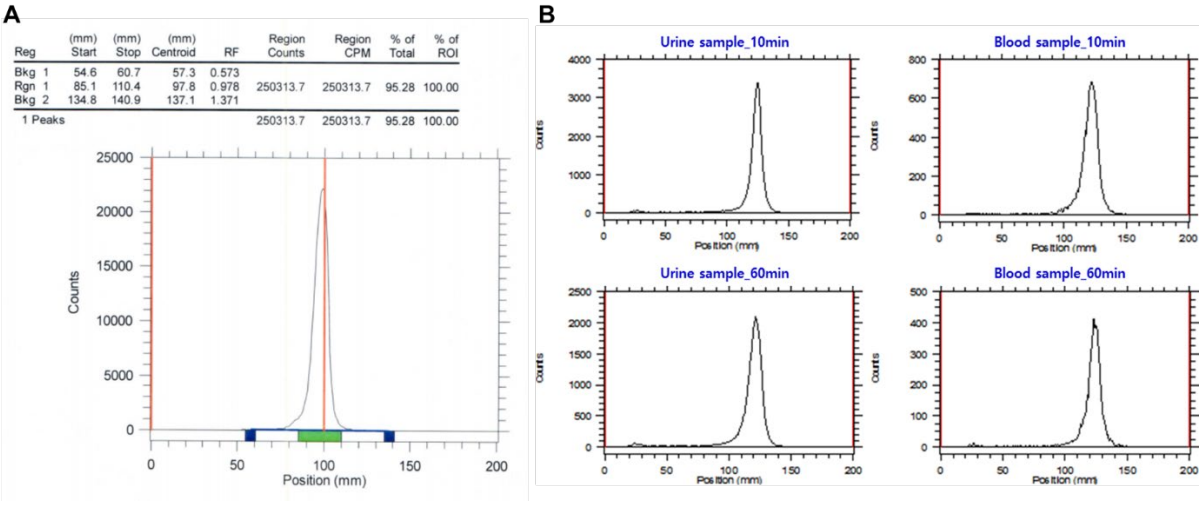

Figure S1. Radiochemical purity was assessed according to the thin layer chromatography (TLC) method using 0.1 M sodium carbonate (Na_2CO_3) solution as a solvent with 1 μL of 68Ga-NGUL. The stability test of ^{68}Ga-NGUL was conducted at baseline, 1 hour, and 2 hours. pH was measured by dropping 1 μL of ^{68}Ga-NGUL on pH paper. Also, the TLC experiment was performed using urine and blood samples 10 minutes, 1 hour after the injection. The radiochemical purity of ^{68}Ga-NGUL was over 95% and remained stable until 2 hours at room temperature (A). pH was measured to be 4.7, this was a value that fits our preset criteria (pH 4 to 5). Furthermore, the radiochemical purities of the compound were over 99% in urine and blood samples which were obtained 10 minutes, 1 hour after the injection (B).

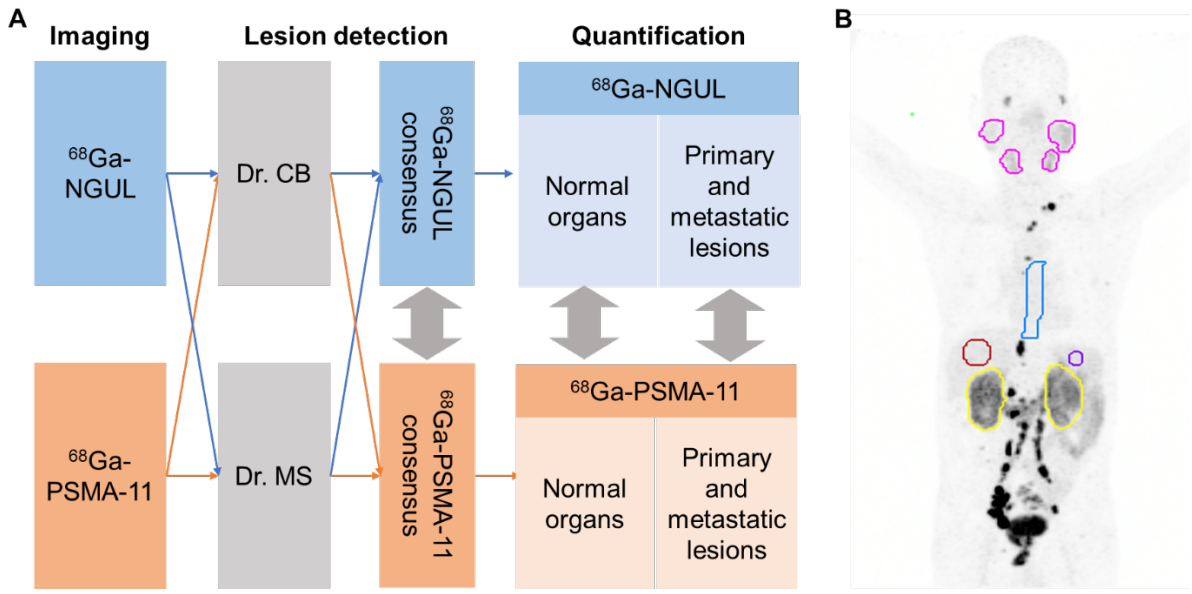

Figure S2. Image acquisition and analysis

(A) Whole patients underwent whole-body static PET/CT imaging, 1 hour after an injection of PSMA targeting tracer with a mean dose of 130.2 ± 25.5 MBq (92.5 – 166.5 MBq). Emission scans were acquired at 2 min per bed using dedicated PET/CT scanners (Biograph mCT 64, Siemens Medical Solutions), followed by CT scans with 120kV and a CARE Dose 4D reference of 50mAs for attenuation correction. PET images were reconstructed by an iterative algorithm (ordered-subset expectation maximization, OSEM). Three patients underwent a dynamic study. Dynamic PET/CT scans were performed over the pelvic region for 60 minutes using a 28-frame protocol (10 frames of 30 s, 5 frames of 60 s, 5 frames of 120 s, and 8 frames of 300 s). Reconstruction parameters were identically applied as the static image. The images were reviewed on MIM software (MIM Encore^{TM}, MIM Software Inc., Cleveland, OH). All scans were reviewed separately by nuclear medicine physicians (CB, MS), masked to the patient medical history. Regarding the inconsistency, we reached a consensus afterward. Both scans were analyzed at a different time point. Any lesion in the prostate was considered as positive when the uptake was focal and higher than adjacent prostate tissue. Outside the prostate, a pathologic lesion was defined as any soft-tissue or skeletal lesion with focal uptake which is higher than normal adjacent tissue and not explained by physiologic uptake. Lesion numbers were counted for both ^{68}Ga-NGUL and ^{68}Ga-PSMA-11. For the quantitative analysis, SUV_{max} of all lesions, up to a maximum of five lesions total (and a maximum of two lesions per organ) with the most intense tracer uptake, were estimated in each patient. The tumor-to-background ratio was measured based on the ratio of tumor SUV_{max} and the gluteal muscle SUV_{mean} reflecting the background activity. (B) Normal tissue distribution was compared in the inferior vena cava and the following organs:

major salivary glands, liver, spleen, and kidney. The volume of interest was applied to major salivary glands and kidneys using a gradient-based segmentation method (PET Edge). Spherical volume of interest was drawn on the liver and spleen. For the evaluation of inferior vena cava, circular regions of interests were drawn on every 5-mm axial image and interpolated to acquire a single volume of interest, from the liver tip to the subcarinal level. In addition, spherical volume of interest was applied to the gluteal muscle to estimate the background activity. The normal-organ distribution and blood pool activity of both tracers were quantified as SUV_{mean}. There was no visual evidence of tumor involvement in the target organs, where the volume of interest was drawn. In addition, three patients underwent dynamic PET scanning (60 min) of the pelvic region and lower abdomen to evaluate the urinary excretion by estimating bladder activity.

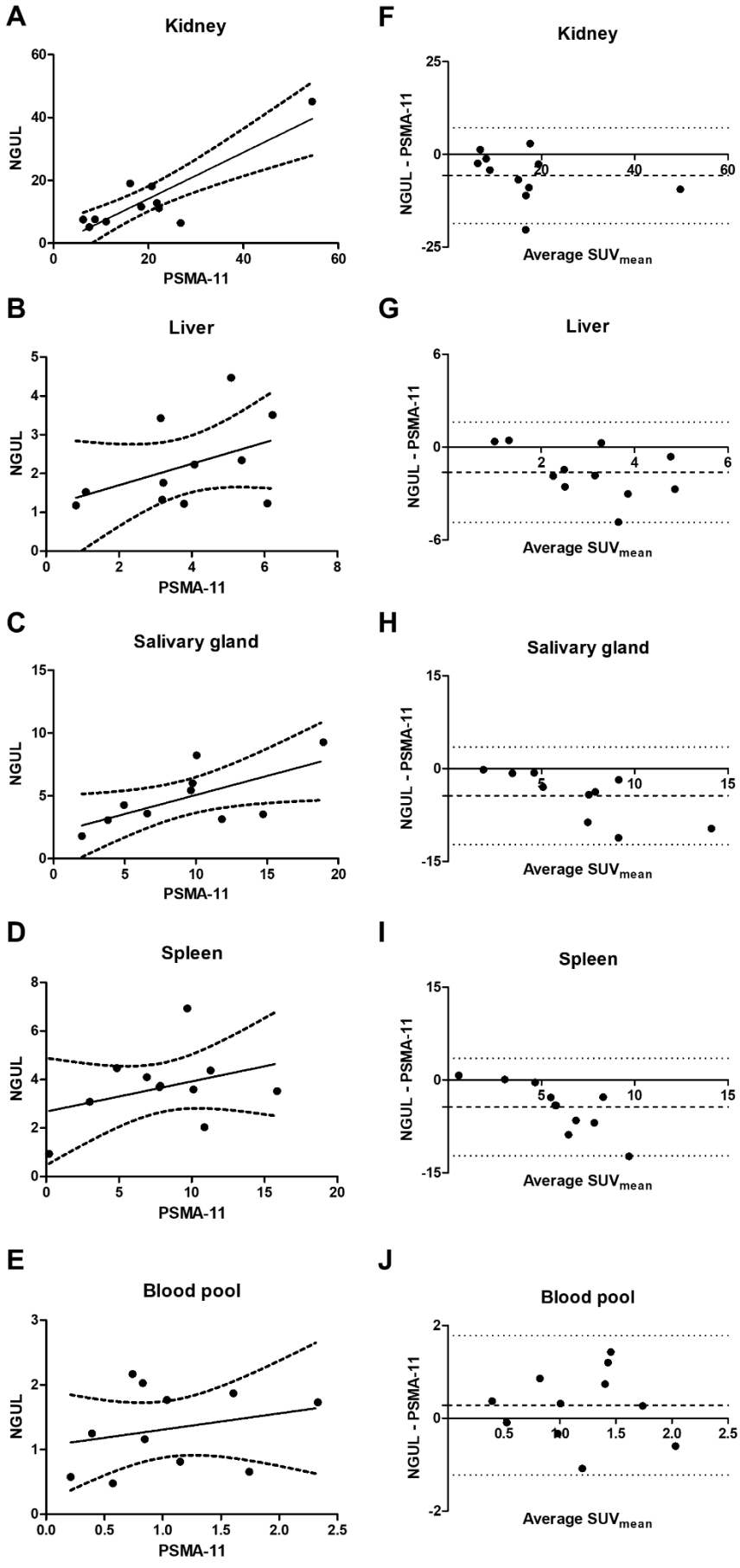
A
Kidney
NGUL
PSMA-11
F
Kidney
NGUL - PSMA-11
Average SUVmean
B
Liver
NGUL
PSMA-11
G
Liver
NGUL - PSMA-11
Average SUVmean
C
Salivary gland
NGUL
PSMA-11
H
Salivary gland
NGUL - PSMA-11
Average SUVmean
D
Spleen
NGUL
PSMA-11
I
Spleen
NGUL - PSMA-11
Average SUVmean
E
Blood pool
NGUL
PSMA-11
J
Blood pool
NGUL - PSMA-11
Average SUVmean

Figure S3. Correlation and agreement between ^{68}Ga-NGUL and ^{68}Ga-PSMA-11 in normal organs

(A-E) Scatter plot of SUV_{mean} showing the correlation between ^{68}Ga-PSMA-11 and ^{68}Ga-NGUL in each normal organ. In the kidney, both tracers showed good correlation, whereas, other organs showed a fair to poor correlation between two tracers. Regression line and 95% CI were plotted. (F-J) Bland-Altman plot showing the difference of SUV_{mean} between ^{68}Ga-PSMA-11 and ^{68}Ga-NGUL, according to their average. Bland-Altman analysis revealed proportional bias in the salivary gland and spleen. Here the difference between ^{68}Ga-NGUL and ^{68}Ga-PSMA-11 uptake increased as the average activity increased. Blood pool activity showed no significant difference between the two tracers. Accordingly, an acceptable agreement with a mean bias of 0.3±0.7 was observed in the blood pool. Dotted lines represent the mean bias and 95% limits of agreement.

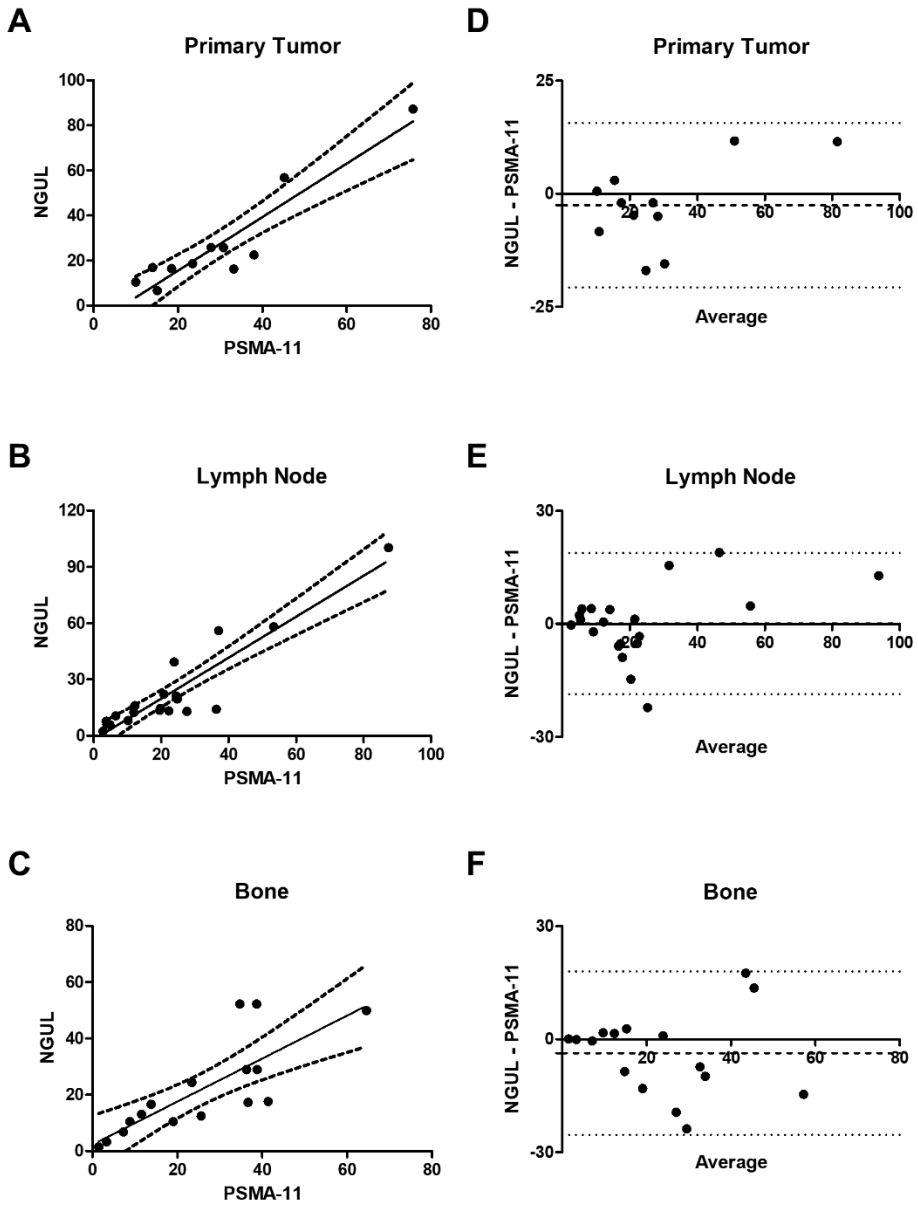

Figure S4. Correlation and agreement between ^{68}Ga-NGUL and ^{68}Ga-PSMA-11 in primary and metastatic lesions

(A-C) Scatter plot of SUV_{max} showing the correlation between ^{68}Ga-PSMA-11 and ^{68}Ga-NGUL in the primary tumor, lymph node metastases, and bone metastases. The quantitative primary tumor uptake showed good correlation between ^{68}Ga-NGUL and ^{68}Ga-PSMA-11 ($R^2 = 0.910$, $p < 0.001$). The quantified uptake in metastatic lesions of both tracers showed a good correlation with R^2 of 0.845 in lymph node

metastases and 0.624 in bone metastases. Regression line and 95% CI were plotted. (D-F) Bland-Altman plot showing the difference of SUV_{max} between ^{68}Ga-PSMA-11 and ^{68}Ga-NGUL, according to their average. The two tracers had an acceptable overall agreement with a calculated mean bias of -3.2 ± 7.2 for the primary tumor, -1.5 ± 10.2 for lymph node metastases, and -4.8 ± 11.2 for bone lesions. Dotted lines represent the mean bias and 95% limits of agreement.

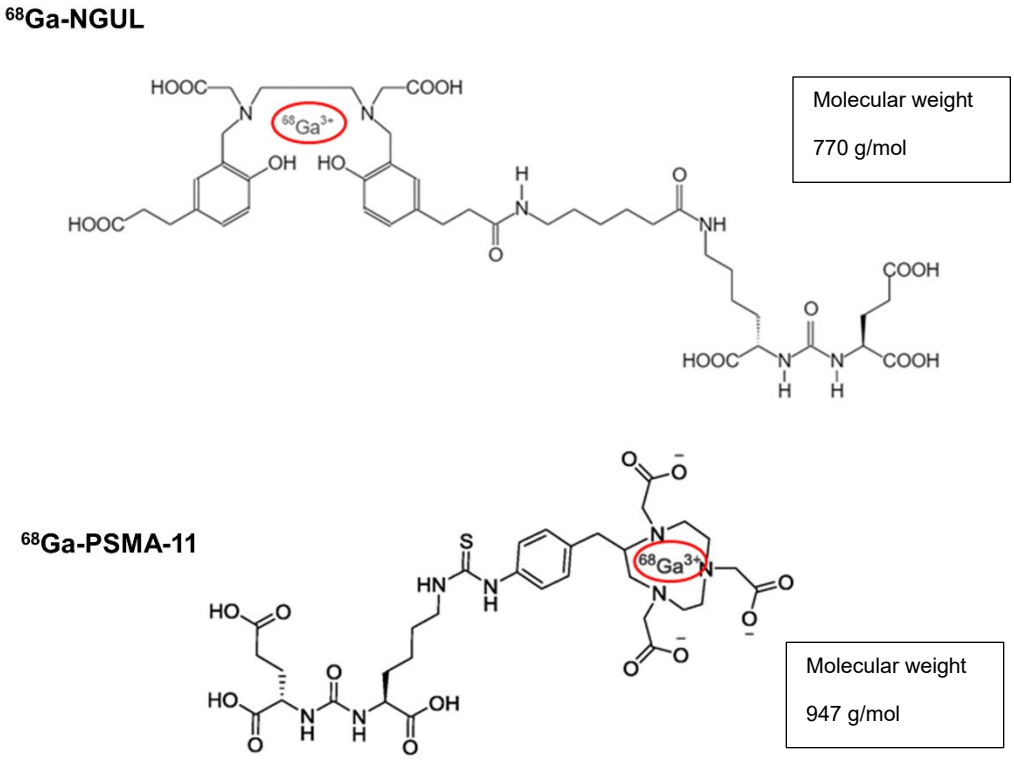

Figure S5. Radiolabeling and chemical structure of ^{68}Ga-NGUL and ^{68}Ga-PSMA-11

The radiolabeling of ^{68}Ga-PSMA-11 was performed over 5 minutes using a disposable cassette, labeling kit, and 10ug of precursor, PSMA-HBED-CC (ABX GmBH, Radeberg, Germany) dissolved in 1 mL of sodium acetate buffer (0.25 M). ^{68}Ga-NGUL was prepared similarly to the previous study (*Bioorg Med Chem*. 2018;26:2501-2507). Briefly, $^{68}GaCl_3$ in 0.1 M HCl solution was added to the NGUL kit vial (Cellbion, Seoul, Korea). The vial was vigorously mixed for 1 min and then was incubated for 10 min at room temperature.

SUPPLEMENTARY TABLES

Table S1. Characteristics of patients (n=11)

	Age	Time gap between both scans (day)	PSA (ng/ml)	Gleasons Score	Local Treatment	Chemotherapy	Hormonal Therapy	Disease State
1	69	1	1.8	N/A	Not done	Not done	Done	HSPC
2	67	4	94.8	4+3	Not done	Done	Done	CRPC
3	67	1	184.6	3+4	TURP	Not done	Done	HSPC
4	70	4	N/A	4+3	Not done	Not done	Done	HSPC
5	72	2	N/A	N/A	Not done	Not done	Done	HSPC
6	50	4	151.0	4+4	Not done	Not done	Done	HSPC
7	55	1	28.3	N/A	Radiotherapy	Done	Not done	CRPC
8	84	1	1.7	3+5	Not done	Not done	Done	HSPC
9	63	1	1462.9	4+5	Not done	Done	Done	CRPC
10	80	2	63.7	3+3	TURP	Not done	Done	HSPC
11	67	4	52.2	4+5	Not done	Done	Not done	CRPC
Median (Range)	**67** (50-84)	**2** (1-4)	**63.7** (1.8-1462.9)					

Table S2. Comparison of quantitative values between ^{68}Ga-NGUL and ^{68}Ga-PSMA-11

Target Organ	**NGUL SUV_{mean}** Median (ICR)	**PSMA-11 SUV_{mean}** Median (ICR)	**Paired test p value**	**Linear Regression** R^2	**Linear Regression** p value	**Bland-Altman** Mean Bias (SD)
Kidney	11.6 (7.8-17.2)	20.7 (10.1-23.1)	0.005	0.775	< 0.001	-6.3 (6.2)
Liver	1.8 (1.5-3.2)	4.0 (3.4-5.3)	0.005	0.184	0.188	-1.8 (1.6)
Salivary gland*	4.4 (3.1-6.9)	9.9 (4.9-12.2)	0.002	0.489	0.024	-4.7 (3.7)
Spleen	3.7 (3.2-4.6)	9.7 (6.3-10.7)	0.005	0.294	0.085	-4.7 (3.9)
Blood pool	1.3 (0.8-1.8)	0.9 (0.8-1.5)	0.240	0.076	0.413	0.3 (0.7)
Target Lesion	**NGUL SUV_{max}**	**PSMA-11 SUV_{max}**				
Primary Tumor	18.7 (16.4-31.8)	27.8 (17.9-38.7)	0.102	0.910	< 0.001	-3.2 (7.2)
Lymph Node	14.8 (10.5-24.8)	20.3 (9.2-26.2)	0.674	0.841	< 0.001	-1.5 (10.2)
Bone	19.6 (11.5-29.0)	24.5 (11.4-37.7)	0.175	0.697	< 0.001	-4.8 (11.2)

*Number of the case is 10, since the scan coverage was limited to the lower neck level

ICR: Interquartile range, SD: Standard deviation

Table S3. Visual analysis of lesion number

Patient	Primary Tumor		Lymph Node		Bone		Total	
	NGUL	PSMA-11	NGUL	PSMA-11	NGUL	PSMA-11	NGUL	PSMA-11
1	Yes	Yes	5	5	13	13	18	18
2	Yes	Yes	27	27	12	12	39	39
3	Yes	Yes	4	4	23	23	27	27
4	Yes	Yes	12	12	disseminated	disseminated	12	12
5	Yes	Yes	14	14	disseminated	disseminated	14	14
6	Yes	Yes	8	8	8	8	16	16
7	Yes	Yes	13	13	0	0	13	13
8	Yes	Yes	5	5	0	0	5	5
9	Yes	Yes	0	0	disseminated	disseminated	0	0
10	Yes	Yes	51	51	3	3	54	54
11	Yes	Yes	22	22	0	0	22	22
Sum	11	11	161	161	59	59	231	231

Table S4. Dosimetry

In order to evaluate the in vivo distribution of ^{68}Ga-NGUL in normal BALB/c mice, blood and major organs were obtained at 15, 30 minutes and 1, 2, 4 hours after intravenous injection of ^{68}Ga-NGUL (185 kBq/100 μL) (n=4 for each time point). Biodistribution data was obtained by calculation of weight and radioactivity of the blood and major organs. The absorbed doses of organs and effective dose were calculated by extrapolating the biodistribution results obtained based on the mouse to a normal adult (70 kg), using the OLINDA/EXM program.

Target organ	Mean(mGy/MBq)
Intestine	0.0036
Stomach wall	0.0036
Heart wall	0.0126
Kidneys	0.2190
Liver	0.0023
Lungs	0.0038
Muscle	0.0016
Red marrow	0.0067
Osteogenic cells	0.0094
Spleen	0.0453
Effective dose	**0.019 (mSv/MBq)**